RSC Advances

Accepted Manuscript

This article can be cited before page numbers have been issued, to do this please use: T. M. W. J. Bandara, H.D.N.S Fernando, M. Furlani, I. Albinsson, M. A. K. L. Dissanayake and B. Mellander, *RSC Adv.*, 2016, DOI: 10.1039/C6RA22335D.

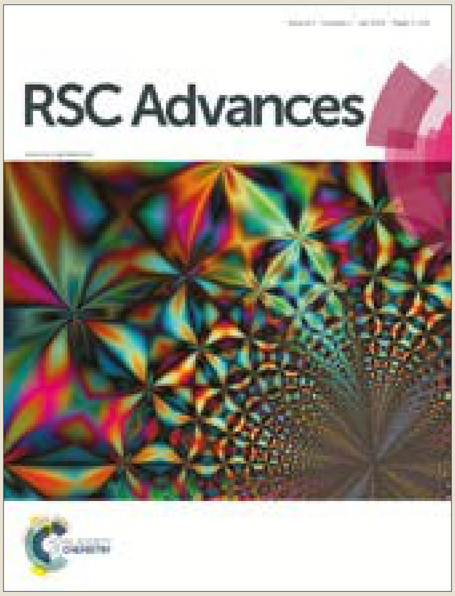

View Article Online
DOI: 10.1039/C6RA22335D

Performance enhancers for gel polymer electrolytes based on LiI and RbI for quasi-solid-state dye sensitized solar cells

T.M.W.J. Bandara[a,b*], H.D.N.S. Fernando[a,b], M. Furlani[c],

I. Albinsson[c] and M.A.K.L. Dissanayake[d], B.-E. Mellander[a]

[a]*Department Physics, Chalmers University of Technology, Gothenburg, Sweden,*

[b]*Department of Physical Sciences, Rajarata University of Sri Lanka, Mihintale, Sri Lanka,*

[c]*Department of Physics, University of Gothenburg, Gothenburg, Sweden,*

[d]*National Institute of Fundamental Studies, Hantana Road, Kandy, Sri Lanka*

Abstract

In this study, the effect of additives (enhancers) on efficiency enhancement in dye sensitized solar cells (DSSCs) containing two series of gel polymer electrolytes, one based on LiI and the other based on RbI have been systematically studied. Polyacrylonitrile (PAN) was used as the host polymer while the performance enhancers used in each case were tetrapropylammoniumiodide (Pr_4NI), the ionic liquid 1-methyl 3-propyl imidazolium iodide (MPII) and 4-tert-butylpyridine (4TBP) respectively. Appropriate amounts of the selected enhancers were incorporated one by one, in LiI based and RbI based gel electrolytes. The incorporation of Pr_4NI and MPII led to an increase in conductivity of the electrolyte, while 4TBP showed a decrease in conductivity. The maximum conductivity of 3.85 mS cm^{-1} at room temperature was shown by the RbI based-series while for the LiI based series the maximum conductivity was 2.95 mS cm^{-1}.

Each of these electrolytes with respective additives was used to fabricate quasi-solid state DSSCs. For the DSSCs based on the LiI containing series, a significant short circuit current density (J_{sc}) enhancement (161%) from 3.65 to 9.54 mA cm^{-2} was observed due to the addition of Pr$_4$NI. This J_{sc} value further increased to 9.7 mA cm^{-2} due to the addition of MPII and 4TBP. For the DSSCs with corresponding Rb based electrolytes with all three additives, the highest J_{sc} value obtained was 11.5 mA cm^{-2}. The incorporation of the three additives Pr$_4$NI, MPII and 4TBP collectively enhanced the open circuit voltages and the efficiencies of both LiI and RbI containing quasi-solid state DSSCs. Another important finding from this work is that, rarely used RbI containing electrolytes have exhibited superior DSSC performance compared to more frequently used LiI based electrolytes. Hence, RbI appears to be a better candidate compared to LiI to fabricate gel polymer electrolytes for DSSCs in general. The three additives have contributed to a remarkable efficiency enchantment in DSSCs by 449.3% for the LiI based electrolyte and by 35.7% for the RbI based electrolyte.

Keywords: Dye sensitized solar cell, alkaline cation, quasi-solid state -electrolyte, PAN, efficiency enhancement.

Introduction

Dye-sensitized solar cells (DSSCs) have gained wide attention owing to their low purity demands on raw materials, simple fabrication methods, relatively good performance and eco-friendly preparation methods etc. [1,2]. Although reasonably good efficiencies have been achieved using liquid electrolytes as ionic conductors [3,4,5], there are problems associated with the use of liquid electrolytes, such as leakage and volatilization of the solvents due to ineffective sealing of the cells, photo-degradation and desorption of the dye as well as corrosion of the counter electrode, limiting the long-term stability [1,6]. These issues in liquid electrolyte based DSSCs can be addressed to a great extent using quasi-solid state or

View Article Online
DOI: 10.1039/C6RA22335D

gel polymer electrolytes [7]. Although, inorganic hole conducting materials substituting the electrolyte have shown excellent performance in recent years, when coupled with methylammonium lead halide perovskites in solar cells, such inorganic as well as organic hole conducting materials have not been effectively used in DSSCs so far [8,9,10,11]. Thus, solid or quasi solid state polymer electrolytes still stand out as promising electrolytes for DSSCs.

Although the performance of the DSSCs with quasi-solid-state or gel electrolytes is lower than that with liquid electrolytes, the quasi-solid electrolytes are a promising alternative to the liquid electrolytes due to improved mechanical, chemical and thermal stability[1,7]. Generally, in gel polymer or solid polymer electrolytes, salts are dissolved in a host polymer matrix. Incorporation of different additives to these polymer electrolytes is important to enhance the ion transport in the electrolyte and subsequent improvement of the performance of the DSSCs. In this work, two series of polyacrylonitrile (PAN) and alkaline iodide based gel electrolyte systems incorporating ethylene carbonate (EC) and propylene carbonate (PC) co-solvents as plasticizers are selected as the reference electrolytes. LiI and RbI are selected as the two iodide salts, especially considering the effects of alkaline cations in the electrolytes on DSSC performance [12]. However, due to the complex nature of the charge transport mechanism in DSSCs, particularly at interfaces, a variety of additives with different functionalities has the ability to enhance the cell efficiency as well as the cell stability. This study is focused on systematically understanding the functions of three selected performance enhancers, tetrapropylammoniumiodide (Pr_4NI), 1-methyl 3-propyl imidazolium iodide (MPII) ionic liquid and 4-tert-butylpyridine (4TBP). The effect of each of these additives on ionic conductivity, fill factor (*ff*), open-circuit voltage (V_{oc}), short-circuit current density (J_{sc}) and efficiency in DSSCs is studied in detail in this work.

View Article Online
DOI: 10.1039/C6RA22335D

The first additive or performance enhancer selected in this work, Pr_4NI, has shown higher efficiencies for quasi-solid state DSSCs compared to other salts in the quaternary ammonium iodide series [13]. Pr_4NI, has also exhibited significant efficiency enhancement in DSSCs when mixed with alkaline iodide electrolytes such as KI [14]. Therefore, Pr_4NI was selected as the first performance enhancer to be incorporated in the LiI based and RbI based DSSC series in the present work.

The second additive, the ionic liquid MPII, is a salt that is in the liquid state at room temperature and can be considered as a liquid electrolyte entirely composed of ions [15]. The melting point of ionic liquids is generally below 100 °C. However, low melting point or room temperature ionic liquids have been widely used in the electrolytes for DSSCs due to their favorable chemical and thermal stability and the tendency to improve solar cell permanence. Although high temperature ionic liquids have also been used in DSSCs, not many reports can be found on such studies since they have shown relatively low room temperature conductivities and low efficiencies [16]. In addition, ionic liquids also can function as alternatives to organic solvents used as plasticizers in DSSC electrolytes [17,18].

The third additive, 4-tert-butylpyridine (4TBP) has generally been used as an additive in liquid-electrolyte-based DSSCs resulting in a considerable enhancement of the V_{OC} and the efficiency of DSSCs [19]. The incorporation of 4TBP can reduce the electron recombination rates [20], cause a negative shift of the conduction band edge of TiO_2 film [21] and enhance electron lifetimes in the conduction band [22], all contributing to performance enhancement in DSSCs. In addition, 4TBP affects the surface charge of TiO_2 by decreasing the amount of adsorbed protons and/or counter ions such as Li^+.

2.0 Experimental

2.1 Materials

View Article Online
DOI: 10.1039/C6RA22335D

LiI, RbI, tetrapropylammoniumiodide (Pr_4NI), Polyacrylonitrile (PAN) (Mw. 150,000), iodine (I_2), ethylene carbonate (EC) and propylene carbonate (PC), all with purity greater than 98%, from Aldrich were used as starting materials. 1-methyl 3-propyl imidazolium iodide ionic liquid (MPII) and 4-tert-butylpyridine (4TBP) (96%) were also purchased from Aldrich. Prior to use PAN was vacuum dried for 24 hours at 50 °C. Other materials were used as received. Conducting glass containing fluorine doped tin oxide (FTO) over-layer of 7 Ω cm^{-2} sheet resistance and the sensitizing dye ruthenium 535-bis TBA (N719 dye) were purchased from Solaronix SA. TiO_2 powders P25 and P90 were obtained from Degussa, Germany.

2.2 Electrolyte preparation

For the preparation of the gel electrolytes the method used by us in a previous work was followed [13,23]. It should be mentioned here that, although we have obtained an efficiency of 3 % for DSSCs with a LiI containing gel electrolyte [23], for the present work we have kept the RbI (Rb^+ and I^- ions) concentration close to its maximum within the solubility limit and equivalent LiI molar concentration. For both series the molar compositions of enhancers were also kept the same. Two separate series of gel polymer electrolyte samples were prepared according to the molar composition given by $(PAN)_{10}(EC)_{25}(PC)_{20}(MI)_{1.2}$ $(I_2)_{0.12}$, one series with MI=LiI and the other with MI=RbI, in order to get a visually uniform, non-flowing gel electrolyte, while keeping the molar concentration of the electrolyte constant. Here PAN represents one monomer of the polymer. Compositions of the prepared electrolytes are given in Table 1. Two separate series of gel electrolytes were prepared with LiI and RbI (represented by MI), by blending relevant amount of Pr_4NI (0.0443 g) and MPII (0.0126 g) into the $(PAN)_{10}(EC)_{25}(PC)_{20}(MI)_{1.2}(I_2)_{0.12}$ electrolyte respectively. 4TBP is incorporated by dissolving 0.0217 g of 4TBP in relevant amount of PC (0.5 M solution of 4TBP in PC). This was done in order to ensure that the molar concentrations of iodide ions and cations in corresponding compositions remain the same.

View Article Online
DOI: 10.1039/C6RA22335D

Table 1 The composition of electrolyte $(PAN)_{10}(EC)_{25}(PC)_{20}(MI)_{1.2}(I_2)_{0.12}$ series. The weight of PAN (0.1 g) and EC (0.4151 g) and PC (0.3851 g) were kept unchanged.

Sample	Salt (MI)	Salt /mg	I_2 /mg	Pr_4NI /mg	MPII /mg	4TBP /mg
LiI	LiI	30.384	5.76	-	-	-
RbI	RbI	48.208	5.76	-	-	-
LiI+Pr_4NI	LiI	30.384	5.76	44.3	-	-
RbI+Pr_4NI	RbI	48.208	5.76	44.3	-	-
LiI+Pr_4NI+MPII	LiI	30.384	5.76	44.3	12.6	-
RbI+Pr_4NI+MPII	RbI	48.208	5.76	44.3	12.6	-
LiI+Pr_4NI+MPII+4TBP	LiI	30.384	5.76	44.3	12.6	21.7
RbI+Pr_4NI+MPII+4TBP	RbI	48.208	5.76	44.3	12.6	21.7

2.3 Fabrication of DSSCs

In order to prepare the TiO_2 photo-anode two layers of TiO_2 were deposited on the conducting glass substrate. The first layer was spin-coated on the FTO substrate using a slurry containing TiO_2 P90 powder. The second layer was coated on the first one with a slurry containing TiO_2 P25 powder using the doctor blade method. The photo-electrode preparation is described in detail in a previous publication [23]. The dye adsorption to the TiO_2 coated glass plate was achieved by immersing the sintered TiO_2 coated glass plates in a 0.5 mM ethanolic solution of the ruthenium 535-bis TBA (N719 dye) while both were initially kept at ~60 °C. After ~24 h dye adsorption at room temperature the TiO_2 electrode was rinsed with acetone to remove the unattached TiO_2 particles and dye molecules before assembling the cell. The prepared gel electrolyte was casted on the dye-sensitized TiO_2 electrode and then a platinum (Pt) coated conducting glass plate (counter electrode) was gently pressed on top of the TiO_2 electrode to

View Article Online
DOI: 10.1039/C6RA22335D

form a DSSC with configuration glass/FTO/dye/TiO_2/electrolyte/Pt/FTO/glass. A minimum of three cells were fabricated and tested for each electrolyte sample in order to check the reproducibility of results.

2.4 Measurements

Complex impedance measurements were performed on electrolyte samples sandwiched between two stainless steel electrodes using a HP 4192A RF impedance analyzer in the 10 Hz – 10 MHz frequency range to obtain the ionic conductivity. Measurements were performed during the decreasing temperature run, from 60 °C to 0 °C. Differential scanning calorimetry (DSC) thermograms were obtained using a Mettler Toledo DSC 30 differential scanning calorimeter. Each sample was scanned between -140 °C and 100 °C with a heating rate of 10 °C min^{-1} on multiple cycles. The glass transition temperatures (T_g) were extracted using the 2nd heating cycle. A flow of nitrogen gas was maintained over the perforated pan to avoid any contact with atmospheric moisture during the measurements.

Fabricated solar cells were illuminated using a LOT-Oriel GmbH solar simulator 1.5 AM, 1000 Wm^{-2} (one sun) and *I-V* characteristics of the cells were obtained using an eDAQ Potentiostat and e-coder. The area of the cell exposed to light was 12 mm^2.

3.0 Results and discussion

3.1 Charge Transport in the Electrolyte

The room temperature conductivities of the two series of gel polymer electrolytes based on LiI and RbI with different additives are shown in Fig. 1. Incorporation of both Pr_4NI and MPII contributes to a conductivity enhancement and the highest conductivity of 3.85 mS cm^{-1} at room temperature is obtained for the RbI containing sample.

View Article Online
DOI: 10.1039/C6RA22335D

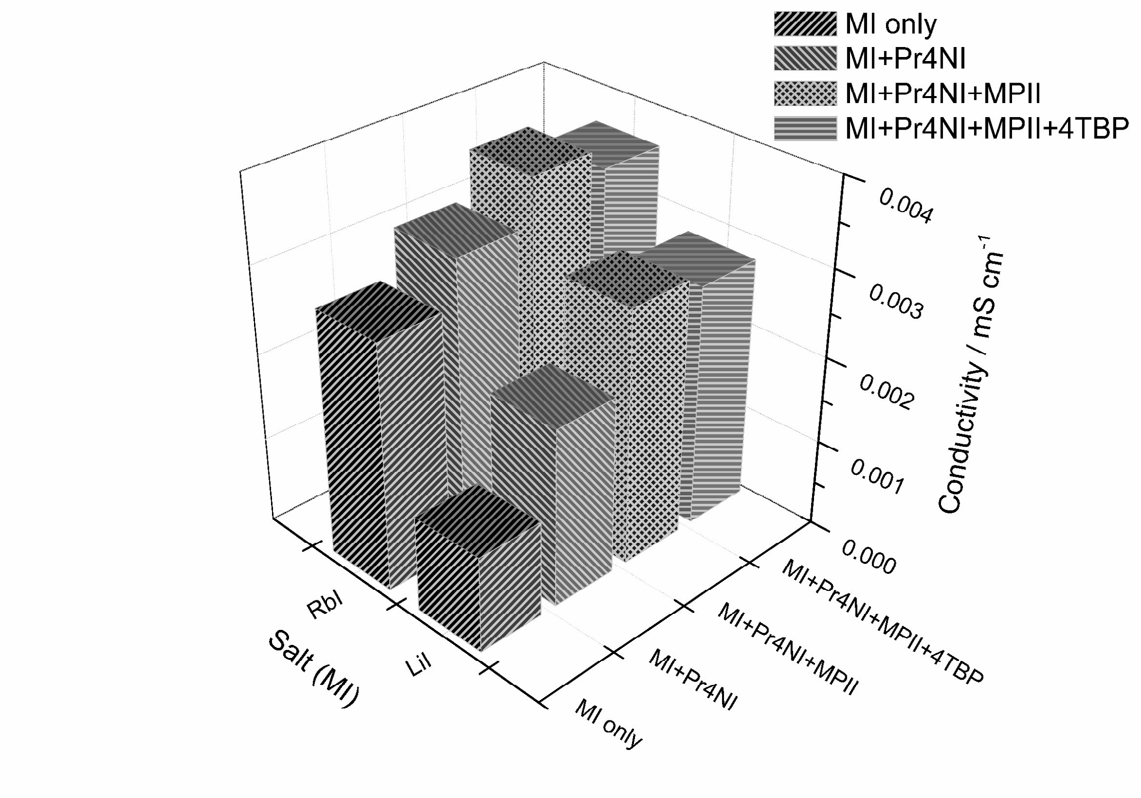

Fig.1. Effect of performance enhancers (additives) on the room temperature ionic conductivity of the two series of gel electrolytes, $(PAN)_{10}(EC)_{25}(PC)_{20}(MI)_{1.2}(I_2)_{0.12}$ where MI=LiI or RbI.

From Fig. 1 it can clearly be seen that for all the LiI containing electrolytes the conductivities are lower than those of the corresponding RbI containing electrolytes. The highest room temperature conductivity of 2.95 mS cm^{-1} of the LiI containing series, is shown by the Pr_4NI and MPII added samples. The highest room temperature conductivity of the RbI containing sample with Pr_4NI and MPII additives is 3.85 mS cm^{-1} which is higher than the corresponding LiI based sample. Both series of electrolytes exhibits a conductivity increase with added Pr_4NI and MPII. Although the highest increase in conductivity due to Pr_4NI and the ionic liquid additives is shown by the LiI based samples, the resulting values are lower than the corresponding conductivity values of the RbI based samples, evidently due to higher conductivity shown by the RbI containing electrolyte with no additives. The trend in conductivity increase due to these two additives remains the same for the entire measured

View Article Online
DOI: 10.1039/C6RA22335D

temperature range (0 - 60 °C) as shown in Fig. 2. This increasing trend can be attributed to the increase of the charge carrier density due to additives. In addition, the ionic liquid can impose a plasticizing effect in the electrolyte increasing the polymer flexibility thus contributing to an increase in the ionic mobility [17,18]. Conversely, a slight drop in conductivity is shown due to the addition of 4TBP to both LiI based and RbI based series which can possibly be the result of a dilution effect. This slight decrease in conductivity with added 4TBP is also common to all measured temperatures.

The conductivity versus 1000/*T* variation for the two electrolyte series based on (PAN) $_{10}$(EC) $_{25}$(PC) $_{20}$(MI)$_{1.2}$(I$_2$)$_{0.12}$ electrolytes where MI=LiI or RbI, with different additives is shown in Figure 2.

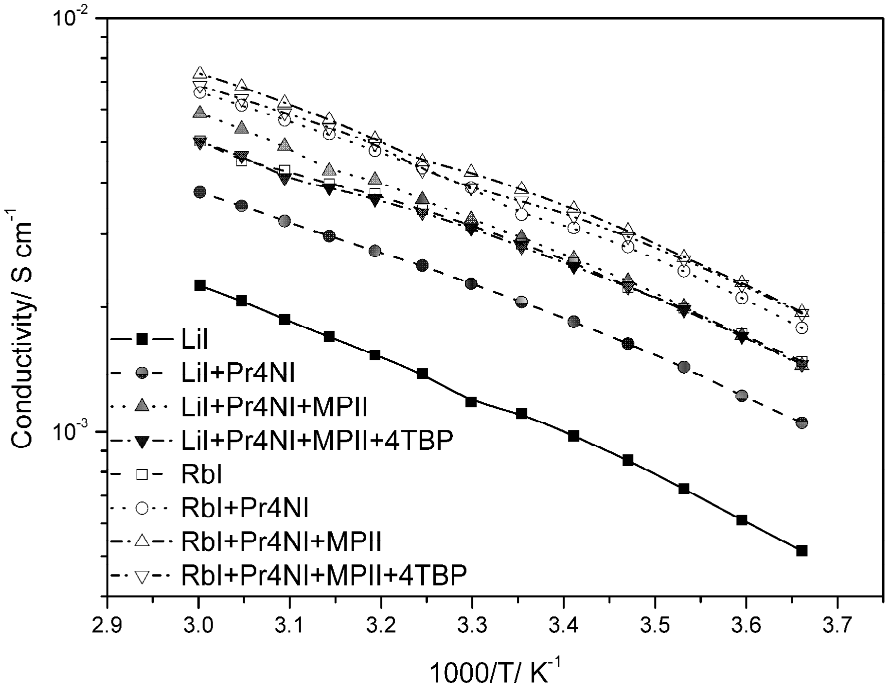

Fig. 2. The conductivity versus 1000/*T* variation for the two electrolyte series based on (PAN) $_{10}$(EC) $_{25}$(PC) $_{20}$(MI)$_{1.2}$(I$_2$)$_{0.12}$ electrolytes where MI=LiI or RbI, with different additives given in Table 1.

View Article Online
DOI: 10.1039/C6RA22335D

The temperature dependence of the conductivity (σ) of all the electrolyte samples show Vogel–Tammann–Fulcher (VTF) behavior and were fitted to the VTF equation,

$$\sigma = AT^{-1/2}\exp\left(-\frac{E_\mathrm{a}}{k_\mathrm{B}(T - T_g{}')}\right) \qquad (1)$$

where σ is the conductivity, T is the absolute temperature, A is a pre-exponential factor, E_a is a pseudo activation energy and $T_\mathrm{g}{}'$ is a reference temperature which is related to the equilibrium state glass transition temperature[24]. The measured glass transition temperature, T_g, was employed as the reference temperature $T_\mathrm{g}{}'$ for the fitting. The appropriateness of the selected T_g is justified by the good fitting shown in Fig. 3 within the measured temperature range. A and E_a values obtained by fitting conductivity data to eq. (1) are given in Table 2. In general, the pre-exponential factor, A, is proportional to the number of free ionic charge carriers in the electrolyte and E_a reveals the energy characteristics [24,25,26]. The difference in E_a values among different electrolyte samples is small. This is expected as the activation energy in both electrolyte series is essentially governed by the PAN polymer matrix and the solvent medium in the gel. However, a somewhat higher value E_a is shown by the LiI containing sample which might be attributed to the drop in ionic mobility resulting from the stronger interactions between Li^+ and electronegative sites in the polymer and plasticizers [23]. Especially, polymer chains can cross-link strongly because of Li^+ due to the high charge density of the cation resulting in a decrease in polymer chain flexibility and thereby increasing the local viscosity of the electrolyte [12].

Charge carries density values and the pseudo activation energy values, derived from Fig. 3 are shown in Table 2 for the electrolyte samples in the two series.

Table 2. The activation energy, E_a, and pre-exponential factor, A, for $(PAN)_{10}(EC)_{25}(PC)_{20}(MI)_{1.2}(I_2)_{0.12}$ electrolytes with different additives.

View Article Online
DOI: 10.1039/C6RA22335D

Sample	***A*/ S m^{-1} K$^{1/2}$**	***E*$_a$/ eV**
LiI	55.19	0.036
Li+Pr$_4$NI	68.43	0.032
LiI+Pr$_4$NI+ MPII	123.99	0.035
LiI+Pr$_4$NI+MPII+4TBP	79.67	0.030
RbI	80.37	0.030
RbI+Pr$_4$NI	125.97	0.033
RbI+Pr$_4$NI+MPII	138.85	0.033
RbI+Pr$_4$NI+MPII+4TBP	118.45	0.032

According to Table 2, the *A* value decreases from 123.99 to 79.67 S m^{-1} K$^{1/2}$ for the LiI based electrolyte containing all three additives and from 138.85 to 118.45 S m^{-1} K$^{1/2}$ for the RbI based electrolyte containing all three additives due to the incorporation of the third additive, 4TBP. The conductivity decrease with added 4TBP may thus be attributed to a decrease of the charge carrier density which in turn can be a result of the dilution effect. In addition, a cation mobility drop may also be possible due to interaction between the cations and the hetero atom in 4TBP. A higher degree of ion dissociation can be expected for the RbI containing electrolytes compared to the LiI containing ones due to the larger size of the Rb$^+$ ion compared to the Li$^+$ ion. This agrees with the higher "*A*" values of the RbI containing samples compared to the corresponding LiI containing samples. In addition, a conductivity drop with added 4TBP can also be attributed to a slower transport of I$^-$/I^{-3} ions as described by Geo et al. using steady-state voltammograms [27].

Variation of ln ($\sigma T^{1/2}$) as a function of 1/(T-T_g) for the $(PAN)_{10}(EC)_{25}(PC)_{20}(MI)_{1.2}(I_2)_{0.12}$ electrolyte series with different additives is shown in Fig. 3.

View Article Online
DOI: 10.1039/C6RA22335D

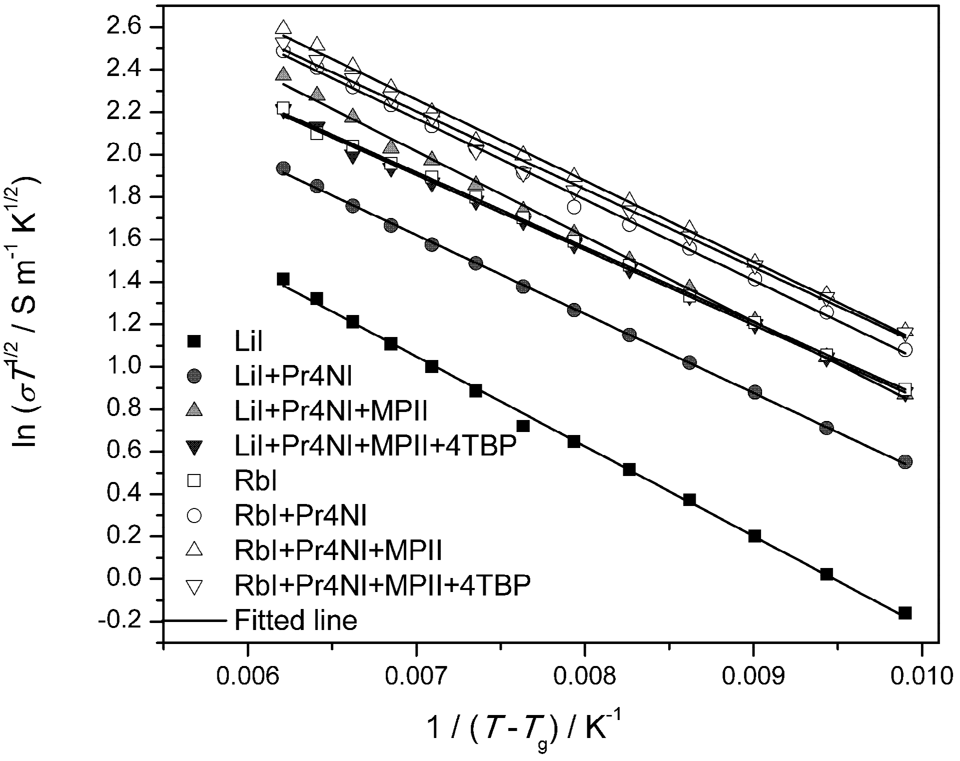

Fig. 3. ln (σ $T^{1/2}$) as function of $1/(T\text{-}T_g)$ for $(PAN)_{10}(EC)_{25}(PC)_{20}(MI)_{1.2}(I_2)_{0.12}$ electrolyte with different additives given in Table 1.

Glass transition temperatures, T_g, for the two $(PAN)_{10}(EC)_{25}(PC)_{20}(MI)_{1.2}(I_2)_{0.12}$ electrolyte series with MI= LiI and RbI containing different additives (given in Table 1) taken for the 1st and 2nd heating cycles are shown in Table 3. According to this Table, T_g values fluctuates around 100 °C. However, these calculated T_g values were used to fit measured conductivity data to the VTF equation.

Table 3. Glass transition temperatures, T_g, for $(PAN)_{10}(EC)_{25}(PC)_{20}(MI)_{1.2}(I_2)_{0.12}$ electrolytes with different additives (given in Table 1) for the 1st and 2nd heating cycles and average values.

Sample	**Onset/ °C**	**mid/ °C**	**onset/ °C**	**mid/ °C**	**average/ °C**
	1st heating		**2nd heating**		
LiI	-101.72	-99.07	-102.95	-100.43	-101.043

View Article Online
DOI: 10.1039/C6RA22335D

RbI	-102.14	-99.13	-102.01	-99.15	-100.608
LiI+Pr_4NI	-103.12	-100.3	-104.27	-101.04	-102.183
RbI+Pr_4NI	-102.29	-98.35	-102.00	-98.63	-100.318
LiI+Pr_4NI+MPII	-101.14	-98.11	-101.38	-98.75	-99.845
RbI+Pr_4NI+MPII	-101.35	-98.62	-101.38	-98.29	-99.910
LiI+Pr_4NI+MPII+4TBP	-103.49	-99.36	-103.71	-100.07	-101.658
RbI+Pr_4NI+MPII+4TBP	-101.32	-97.16	-101.07	-97.00	-99.137

3.2 DSSC Characterization

Two series of DSSCs fabricated using LiI and RbI based electrolytes according to the compositions given in Table 1 were characterized and the resulting photocurrent density and power density versus cell potential (J-V) curves are shown in Fig. 4 and Fig. 5 respectively. Using the J-V characteristic curves shown in Fig 4 and 5, the fill factor (*ff*), the short circuit current density (J_{sc}), the open circuit voltage (V_{oc}) and the power conversion efficiency were calculated for all the DSSCs.

View Article Online
DOI: 10.1039/C6RA22335D

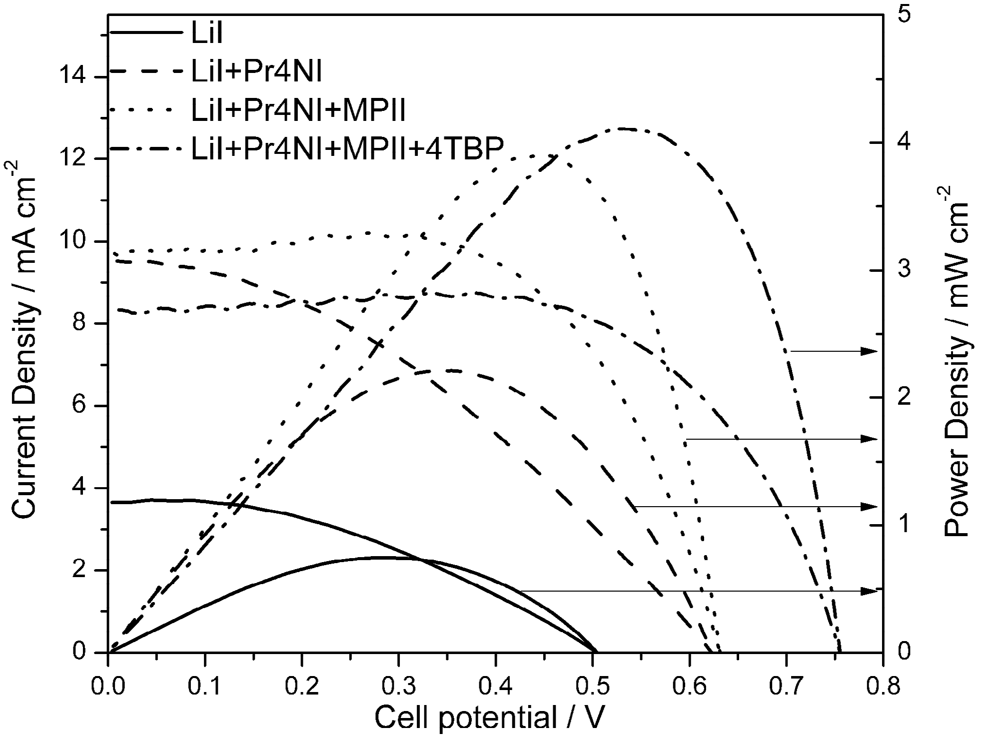

Fig. 4. The photocurrent density (*J-V*) and power density as a function of cell potential in dye sensitized solar cells containing $(PAN)_{10}(EC)_{25}(PC)_{20}(LiI)_{1.2}(I_2)_{0.12}$ electrolyte with different additives given in Table 1. Measurements were taken under irradiation of 1000 W m^{-2} (1.5 AM).

View Article Online
DOI: 10.1039/C6RA22335D

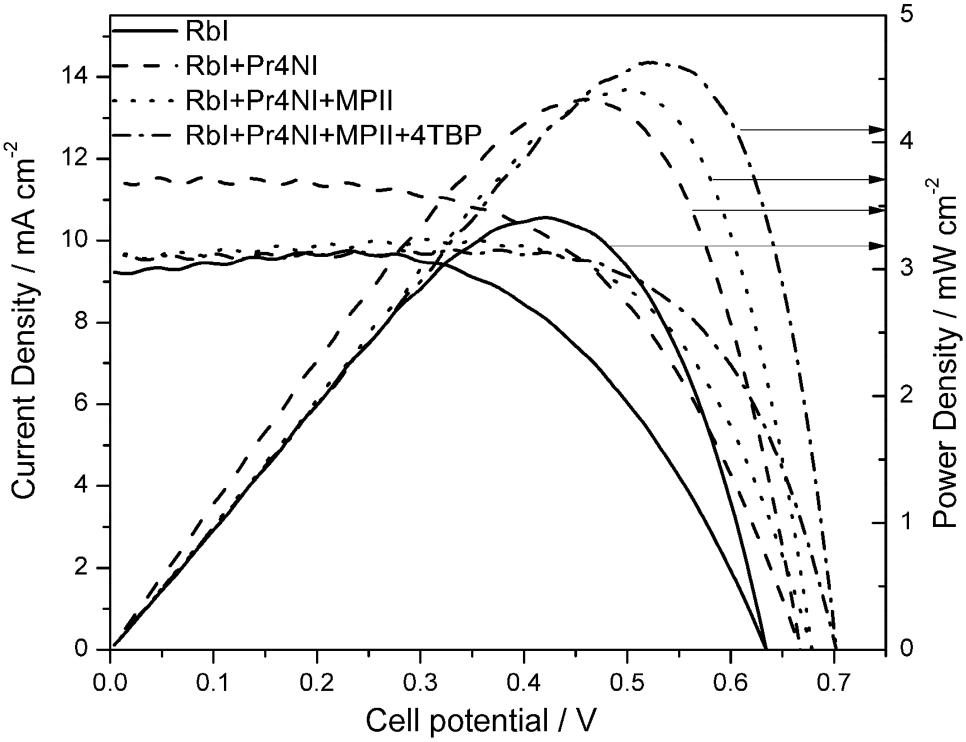

Fig. 5. The photocurrent density and power density (*J-V*) as a function of cell potential in dye sensitized solar cells containing $(PAN)_{10}(EC)_{25}(PC)_{20}(RbI)_{1.2}(I_2)_{0.12}$ electrolyte with different additives given in Table 1. Measurements were taken under irradiation of 1000 W m^{-2} (1.5 AM).

3.2.1 The Effect of Enhancers on the Fill Factor

The fill factor, *ff,* was calculated using the equation,

$$ff = \frac{J_{\mathrm{opt}}\ V_{\mathrm{opt}}}{J_{\mathrm{SC}}\ V_{\mathrm{OC}}} \tag{2}$$

where, J_{opt} and V_{opt} are the current density and voltage at maximum power density. The fill factor of the DSSCs fabricated with these two series of gel electrolytes with different additives are shown in Fig. 6-a. It can be observed that the values are higher for the RbI

View Article Online
DOI: 10.1039/C6RA22335D

containing samples and that the incorporation of Pr_4NI leads to a drop in *ff* values for both sets of electrolytes. The other two additives, MPII and 4TBP, show an increase in the fill factor.

The fill factor represents the ideal quadratic nature of the *J-V* curve and it thus affects the maximum power density (peak power density values in Fig 4 and 5) which determines the power conversion efficiency. In order to attain a higher fill factor in an equivalent circuit model a lower series resistance and a higher shunt resistance that reduces back electron transfer are important [28,29]. The highest *ff* for the LiI and RbI containing DSSC series are 65.2% and 68.6% respectively and these are obtained for the samples with all the three enhancers. The series resistance in a DSSC is mainly caused by the resistance of the electrolyte medium [30]. It is expected that the series resistance decreases with the addition of

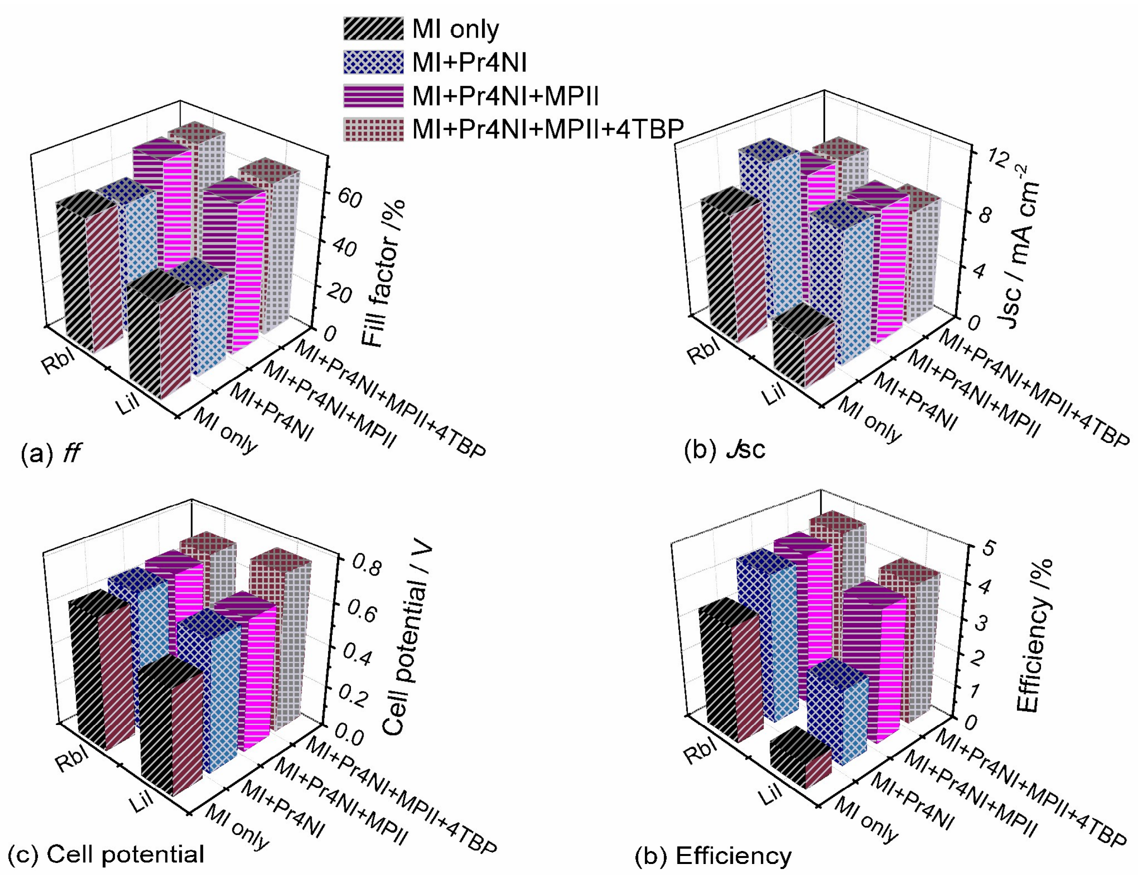

DOI: 10.1039/C6RA22335D

Fig. 6. (a) The fill factor (*ff*), (b) Open circuit voltages (V_{oc}), (c) Short circuit current densities (J_{sc}) and (d) efficiency of the two series of solar cells containing $(PAN)_{10}(EC)_{25}(PC)_{20}(MI)_{1.2}(I_2)_{0.12}$ electrolyte with different additives given in Table 1. Measurements were taken under irradiation of 1000 W m^{-2} (1.5 AM).

Pr_4NI and MPII since the electrolyte conductivity increases with these two enhancers, and the electrolyte thickness is kept unchanged. Even though the addition of 4TBP results a decrease in electrolyte conductivity, the shunt resistance may increase contributing to the fill factor enhancement. Consequently, the highest *ff* is recorded by the DSSC with electrolyte sample, RbI+Pr_4NI+ MPII +4TBP, (ternary iodides and 4TBP) out of all the cells. The double layer capacitance at the TiO_2 /electrolyte interface in particular for the large Rb^+ and by the functionality of the even larger 1-methyl 3-propyl imidazolium cations and also by 4TBP may also contribute to the observed increase in *ff* values [28,29].

3.2.2 The Effect of Enhancers on the Short Circuit Current Density

The short circuit current densities (J_{sc}) of the DSSCs fabricated with these two series of gel electrolytes with different additives are shown in Fig. 6-b. These J_{sc} measurements were done under irradiation of a 1000 W m^{-2}.

It can be clearly seen from this figure that the J_{sc} values of the DSSCs made with RbI containing samples are higher than the cells made with the corresponding LiI containing electrolytes. Better ionic dissociation due to large cation size leading to a larger number of iodide ions compared to the corresponding LiI based electrolytes, appears to contribute to higher J_{sc} values in DSSCs with RbI containing samples [12]. This is consistent with our findings from higher pre-factor, *A,* in these electrolytes as already discussed in section. The incorporation of Pr_4NI additive alone in the electrolytes has contributed to enhance the J_{sc} values to 9.54 mA cm^{-2} and 11.5 mA cm^{-2} respectively for the cells with LiI and RbI containing electrolytes. However, the recorded J_{sc} value for the RbI+Pr_4NI cell, is the highest

View Article Online
DOI: 10.1039/C6RA22335D

obtained in this study. The addition of MPII to these electrolytes has contributed to a decrease of the J_{sc}, possibly due to decrees of iodide ion transport due higher concentration of large size cations Rb^+.

For the LiI containing series of DSSCs, a remarkable J_{sc} enhancement of 161%, from 3.65 to 9.54 mA cm^{-2}, is observed due to the addition of Pr_4NI. This can be ascribed to the conductivity enhancement from 1.11 to 2.06 mS cm^{-1} observed for the LiI electrolyte due to the incorporation of Pr_4NI as shown in Fig 1. The small further J_{sc} enhancement seen for the ternary iodide system can also be attributed to the conductivity enhancement with added MPII. Therefore, the highest J_{sc} of 9.7 mA cm^{-2} for the LiI series is obtained for the ternary iodide system.

For the RbI based electrolyte series the addition of 4TBP has an insignificant influence (a slight drop) for J_{sc} but for the Li series a drop from 9.7 to 8.32 mA cm^{-2} is observed. The decrease of J_{sc} caused by incorporated 4TBP can be attributed to the reduction of the electron injection driving force from the lowest unoccupied molecular orbital (LUMO) of the dye into the conduction band of TiO_2, which is shifted toward higher energy by the added TBP as reported earlier [31,32, 33]. In addition, this J_{sc} drop can also be attributed to the interaction between 4TBP and the coordinated carboxylic groups of the dye through hydrogen bonds which hinders the electron injection from the dye to TiO_2, as described in detail by Zhang et al. for N3 dye [33]. The reduction of J_{sc} with added 4TBP can also to some extent be due to the drop in ionic conductivity as shown in Fig. 1 and Fig. 2 since the J_{sc} of this type of DSSC is governed by ionic conductivity in the electrolyte and in particular by the I^-/I^{-3} concentration and their mobility.

3.2.3 *The Effect of Enhancers on the Open Circuit Voltage*

DOI: 10.1039/C6RA22335D

The open circuit voltage (V_{oc}) of the DSSCs for the two series of gel electrolytes are shown in Fig. 6-c. All the additives, Pr_4NI, MPII and 4TBP have contributed to an increase in V_{oc} in these two series of solar cells. Thus, the highest V_{oc} values for the DSSCs made with LiI and RbI containing series, 756 and 702 mV respectively, are shown for the electrolyte samples with all three additives. Subsequently, the highest V_{oc} recorded in this work is shown by the DSSC with LiI+Pr_4NI+MPII+4TBP as the electrolyte. A significant V_{oc} enhancement can be seen for the LiI series based DSSCs due the addition of 4TBP. However, all the other LiI containing samples show lower V_{oc} values compared to corresponding DSSCs containing RbI. However, the addition of of Pr_4NI and 4TBP have made a remarkable V_{oc} enhancement for the LiI containing cells. Incorporation of Pr_4NI increased the V_{oc} from 504 to 624 mV and 4TBP increased it from 630 to 756 mV for the LiI containing cells. Thus Pr_4NI and 4TBP have both contributed to 23.8% and 20.0% V_{oc} enhancements for the DSSCs with LiI containing electrolyte series. The contribution of 4TBP for the V_{oc} enhancement can be attributed to suppression of the back electron transfer in TiO_2 which is attained by passivating recombination centers with 4TBP as revealed by others using liquid electrolyte based cells[19,21,34]. For example, Nazeeruddin et al. reported about 5.5×10^4 fold decrease in the rate constant for triiodide reduction with added 4TBP [19]. In addition, conduction band edge movement with added 4TBP can contribute to the enhancement of V_{oc}. For instance, the surface treatment of the dye-covered TiO_2 with 4TBP and NH_3 is reported to produce significant band edge movement resulting in a V_{oc} enhancement in DSSCs [20, 21].

In addition, the increase in V_{oc} can be understood by studying the quasi-Fermi level (QFL) of the photo electrode using a three electrode configuration for DSSCs as investigated by Zhang et al. [32]. In that work the effect of 4-tert-butylpyridine (TBP) is attributed to the shift of the quasi-Fermi level (QFL) of dye-sensitized TiO_2 films. The QFL of the TiO_2 films are reported to shift to higher potentials with increasing TBP concentration resulting in an

View Article Online
DOI: 10.1039/C6RA22335D

increase of the V_{oc} in the DSSC [18,32]. Finally we can conclude that all the additives have contributed to gradually increase the V_{oc} for DSSCs with both series of electrolytes. For the RbI based series the V_{oc} enhancement is about 11% whereas for the LiI series, it is high as 50%.

3.2.4 *The Effect of Enhancers on the Cell Efficiency*

The power conversion efficiencies of dye sensitized solar cells fabricated with the two LiI based and RbI based series of gel electrolytes containing different additives are shown in Fig. 6-d. The obtained efficiencies without enhancers, 0.75% for LiI and 3.41% for RbI are in good agreement with previously reported values using a similar electrolyte [12]. In addition, Tennakone *el al* [35] have also observed the lowest solar cell efficiency of 2% for LiI whereas CsI shows an efficiency of 5% under 100 W cm^{-2} irradiation using the same PAN based electrolyte. However, at the irradiation of 1000 W cm^{-2} (Which used in present work), Li, Na K and Cs based cell have shown efficiencies of 0.4, 0.6, 0.9 and 1.9% but authors have used a different electrolyte composition without the enhancers used in this work [35]. In our work a clear trend of increase in cell efficiency is shown by both the series of samples containing LiI and RbI with the incorporation of all three additives. For the DSSC series containing LiI electrolytes, the highest energy conversion efficiency is 4.12% and obtained with the sample containing all three additives, whereas the DSSC with LiI based electrolyte without any additive gives the lowest efficiency of 0.75%. Thus the additives have contributed to a remarkable efficiency enhancement of about 449% for the LiI series.

For the DSSCs fabricated with the RbI based series of electrolytes, the highest power conversion efficiency of 4.63%, is shown by the solar cell with RbI, Pr_4NI, MPII and 4TBP containing electrolyte , whereas the lowest efficiency of 3.41% for this series, is shown by the cell without any additives in the electrolyte. Thus the additives have contributed to efficiency enhancement of about 36% for the RbI series.

View Article Online
DOI: 10.1039/C6RA22335D

Finally, it can be concluded that the additives Pr_4NI, MPII, and 4TBP increase the efficiency of quasi-solid state DSSCs fabricated with both the LiI and RbI containing electrolytes. However, according to our results, the rarely used RbI containing electrolytes offer superior DSSC performance compared to that of the more widely used LiI containing electrolytes. Hence, RbI is a good candidate salt for fabrication of polymer electrolytes for DSSCs. Also, all the additives used in this study are suitable for enhancing the efficiency in quasi-solid state DSSCs.

4.0 Conclusions

LiI and RbI based gel polymer electrolytes are investigated with the intention of improving the performance of N719 sensitized solar cells. Appropriate amounts of selected additives Pr_4NI, MPII and 4TBP were incorporated one by one to $(PAN)_{10}(EC)_{25}(PC)_{20}(MI)_{1.2}(I_2)_{0.12}$ electrolyte series with MI=LiI and MI=RbI. The incorporation of Pr_4NI and MPII led to a conductivity increase whereas, the added 4TBP led to a decreased ionic conductivity. The maximum room temperature conductivity of 3.85 mS cm^{-1} was shown by the RbI based-series while the corresponding value for the LiI series was 2.95 mS cm^{-1}.

Both series of electrolytes were used to fabricate quasi-solid state DSSCs. The *ff* of the solar cells was improved by the additives except for the small drop observed with added MPII. For the LiI containing series a very significant J_{sc} enhancement of 161% from 3.65 to 9.54 mA cm^{-2} was observed when Pr_4NI is incorporated. Subsequently, the highest J_{sc} obtained for the DSSCs made with LiI and RbI electrolyte series were 9.7 and 11.5 mA cm^{-2} respectively.

The additives Pr_4NI, MPII, and 4TBP enhanced the efficiency as well as the V_{oc} of quasi-solid state DSSCs for both the LiI and RbI electrolytes. The efficiency enhancement was about 449% for the LiI series and 36% for the RbI series. In particular, the RbI containing electrolytes offer a superior DSSC performance compared to that of LiI containing electrolytes. Each and every additive employed in this study has enhanced the efficiency and

V_{oc} of the cells thus confirming their suitability for enhancing the efficiency in quasi-solid state DSSCs.

Acknowledgements

Authors wish to acknowledge the research support provided by Swedish Research Council, Chalmers University of Technology Sweden, Carl Tryggers Foundation for Scientific Research and National Research Council of Sri Lanka.

References

1. J. Wu, Z. Lan, J. Lin, M. Huang, Y. Huang, L. Fan and G. Luo, Electrolytes in Dye-Sensitized Solar Cells, Chem. Rev., 2015, **115**, 2136-2173
2. F. Bella, C. Gerbaldi, C. Barolob and M. Gratzel, Aqueous dye-sensitized solar cells, 2015, **44**, 3431-3473.
3. L. Han, N. Koide, Y. Chiba, A. Islam, R. Komiya, N. Fuke, A. Fukui and R. Yamanaka, Improvement of efficiency of dye-sensitized solar cells by reduction of internal resistance. Appl. Phys. Lett., 2005, **86**, 213501.
4. A. Yella, H.W. Lee, H. N. Tsao, C. Yi, A.K. Chandiran, M. K. Nazeeruddin, E. W. G. Diau, C. Y. Yeh, S. M. Zakeeruddin and M. Grätzel, Porphyrin-sensitized solar cells with cobalt (II/III)-based redox electrolyte exceed 1_2 percent efficiency. Science, 2011, **334** (6056):629-634.
5. K. Kakiage, Y. Aoyama, T. Yano, K. Oya, J. Fujisawa and M. Hanaya, Chem. Commun., 2015, **51**, 15894-15897
6. H. Tributsch, Dye sensitization solar cells: a critical assessment of the learning curve, Coordination Chemistry Reviews, 2004, **248**, 1511-1530.

View Article Online
DOI: 10.1039/C6RA22335D

7. F. Bella and R. Bongiovanni, Photoinduced polymerization: An innovative, powerful and environmentally friendly technique for the preparation of polymer electrolytes for dye sensitized solar. Review J. Photochem Photobio C:Photochemistry, 2013, **16**, 1-21.
8. A. M. Green, A. Ho-Baillie and H. J. Snaith, The emergence of perovskite solar cells, Nature Photonics, 2014, **8**, 506-524.
9. Q.-B. Meng, K. Takahashi, X.-T. Zhang, I. Sutanto, T. N. Rao, O. Sato, and A. Fujishima, Fabrication of an Efficient Solid-State Dye-Sensitized Solar Cell, Langmuir, 2003, **19**, 3572-3574.
10. S. Moribe, A. Takeichi, J. Seki, N. Kato, K. Higuchi, K. Ueyama, K. Mizumoto and T. Toyoda, Improved Performance of Solid-State Dye-Sensitized Solar Cells with CuI: Structure Control of Porous TiO_2 Films, Applied Physics Express, 2012, **5** (11) 2302.
11. T. Malinauskas, D. Tomkute-Luksiene, Ru Sens, M. Daskeviciene, R. Send, H. Wonneberger, V. Jankauskas, I. Bruder and V. Getautis, Enhancing Thermal Stability and Lifetime of Solid-State Dye- Sensitized Solar Cells via Molecular Engineering of the Hole- Transporting Material Spiro-OMeTAD, ACS Appl. Mater. Interfaces, 2015, **7**, 11107-11116.
12. T. M. W. J. Bandara, H. D. N. S. Fernando, M. Furlani, I. Albinsson, M. A. K. L. Dissanayake, J. L. Ratnasekera and B.-E. Mellander, Effect of the alkaline cation size on the conductivity in gel polymer electrolytes and their influence on photo electrochemical solar cells, Phys. Chem. Chem. Phys., 2016, **18**(16), 10873-10881.

13 T. M. W. J. Bandara, W. J. M. J. R. Jayasundara, M. A. K. L. Dissanayake, M. Furlani, I. Albinsson and B.-E Mellander, Effect of cation size on the performance of dye sensitized nanocrystalline TiO_2 solar cells based on quasi-solid state PAN electrolytes containing quaternary ammonium iodides, Electrochimica Acta, 2013, **109**, 609-616.

View Article Online
DOI: 10.1039/C6RA22335D

14 M. A. K. L. Dissanayake, C. A. Thotawatthage, G. K. R. Senadeera,, T. M. W. J. Bandara, W. J. M. J. S. R. Jayasundera and B.-E. Mellander, Journal of Photochemistry and Photobiology A: Chemistry, 2012, **246**, 29– 35.

15. R. D. Rogers and K. R. Seddon, Ionic Liquids- Solvents of the Future, Science 2003, **302**, 792-793.

16. T. M. W. J. Bandara, P. Ekanayake, M. A. K. L. Dissanayake, I. Albinsson and B.-E. Mellander, A polymer electrolyte containing ionic liquid for possible applications in photoelectrochemical solar cells, J. Solid State Electrochemistry, 2010, **14**,1221–1226.

17. M. Gorlov and L. Kloo, Dalton Trans. 2008, **28** (20), 2655-66.

18. T. Stergiopoulos, M. Konstantakou and P. Falaras, Dye solar cells combining a TiO_2 surface-blocking organic sensitizer and solvent-free ionic liquid-based redox electrolyte, RSC Adv., 2013, **3**, 15014–15021.

19. K. Nazeeruddin, A. Kay, I. Rodicio, R. Humphry-Baker, E. Mueller, P. Liska, N. Vlachopoulos and M. Gratzel, Conversion of Light to Electricity by cis-XzBis(2,2'-bipyridyl-4,4'-dicarboxylate)ruthenium(11) Charge-Transfer Sensitizers (X = C1-, Br-, I-, CN-, and SCN-) on Nanocrystalline TiO_2 Electrodes, J. Am. Chem. Soc., 1993, **115**, 6382.

20. S. Huang, G. Schlichthorl, A. Nozik, M. Gratzel and A. Frank, Charge Recombination in Dye-Sensitized Nanocrystalline TiO_2 Solar Cells, J. Phys. Chem. B, 1997, **101**, 2576.

21. G. Schlichthorl, S. Huang, J. Sprague and A. Frank, J. Phys. Chem. B, 1997, **101**, 8141.

22. G. Boschloo, L. Haggman and A. Hagfeldt, J. Phys. Chem. B, 2006, **110**, 13144-50.

23. T. M. W. J. Bandara, W. J. M. J. S. R. Jayasundara, H. D. N. S. Fernado, M. A. K. L. Dissanayake, L. A. A. De Silva, P. S. L. Fernando, M. Furlani and B.-E. Mellander, Efficiency enhancement of dye-sensitized solar cells with PAN:CsI:LiI quasi-solid state (gel) electrolytes, J. Appl. Electrochem. 2014, **44**, 917–926.

View Article Online
DOI: 10.1039/C6RA22335D

24. Y.-J. Wang, Y. Pan, L. Wang, M.-J. Pang and L. Chen, J. Applied Polymer Science, 2006, **102**, 4269–4275.
25. W. S. Lee, D. W. Kim, C. Lee, S. I. Woob and Y. Kang, J. Electrochem. Sci. Tech. 2011, **2**-1, 26-31.
26. J. R. M. Giles, Solid State lonics, 1987, **24**, 155-167.
27. R. Gao, L. Wang, Y. Geng, B. Ma, Y. Zhu, H. Dong and Y. Qiu, Interface modification effects of 4-tertbutylpyridine interacting with N3 molecules in quasi-solid dye-sensitized solar cells, Phys. Chem. Chem. Phys., 2011, **13**, 10635–10640.
28. R Guliani, A. Jain and A. Kapoor, Exact analytical analysis of dye-sensitized solar cell: Improved method and comparative study, J Open Renewable Energy 2012, **5**, 49-60
29. S. Sarker, H. W. Seo, D. M. Kim. Calculating current density-voltage curves of dye-sensitized solar cells: A straight-forward approach, Journal of Power Sources 2014, **248**, 739-744.
30. G. Boschloo, H. Lindström, E. Magnusson, A. Holmberg and A. Hagfeldt, Optimization of dye-sensitized solar cells prepared by compression method, Journal of Photochemistry and Photobiology A: Chemistry, 2002, **148**, 11–15.
31. G. Boschloo, L. Ha1ggman and A. Hagfeldt, Quantification of the Effect of 4-tert-Butylpyridine Addition to I^-/I^{3-} Redox Electrolytes in Dye-Sensitized Nanostructured TiO2 Solar Cells, J. Phys. Chem. B, 2006, 110, 13144.
32. S. Zhang, M. Yanagida, X. Yang and L. Han, Effect of 4-tert-Butylpyridine on the Quasi-Fermi Level of Dye-Sensitized TiO_2 Films, Appl. Phys. Express, 2011, **4**, 42301-3.
33. K. Zhang, S. Zhang, K. Sodeyama, X. Yang, H. Chen, M. Yanagida, Y. Tateyama, and L. Han, A New Factor Affecting the Performance of Dye-Sensitized Solar Cells in the Presence of 4-tert-Butylpyridine, Applied Physics Express, 2012, **5**, 042303-3.

View Article Online
DOI: 10.1039/C6RA22335D

34. M. Gratzel and K. Kalyanasundaram, Artificial Photosynthesis: Efficient Dye-Sensitized Photoelectrochemical Cells for Direct Conversion of Visible-Light to Electricity, Curr. Sci., 1994, **66**, 706-714.

35. K. Tennakone, G. K. R. Senadeera, V. P. S. Perera, I. R. M. Kottegoda, and L. A. A. De Silva Dye-Sensitized Photoelectrochemical Cells Based on Porous SnO_2/ZnO Composite and TiO_2 Films with a Polymer Electrolyte, Chem. Mater., 1999, **11**(9), 2475-247.

View Article Online
DOI: 10.1039/C6RA22335D

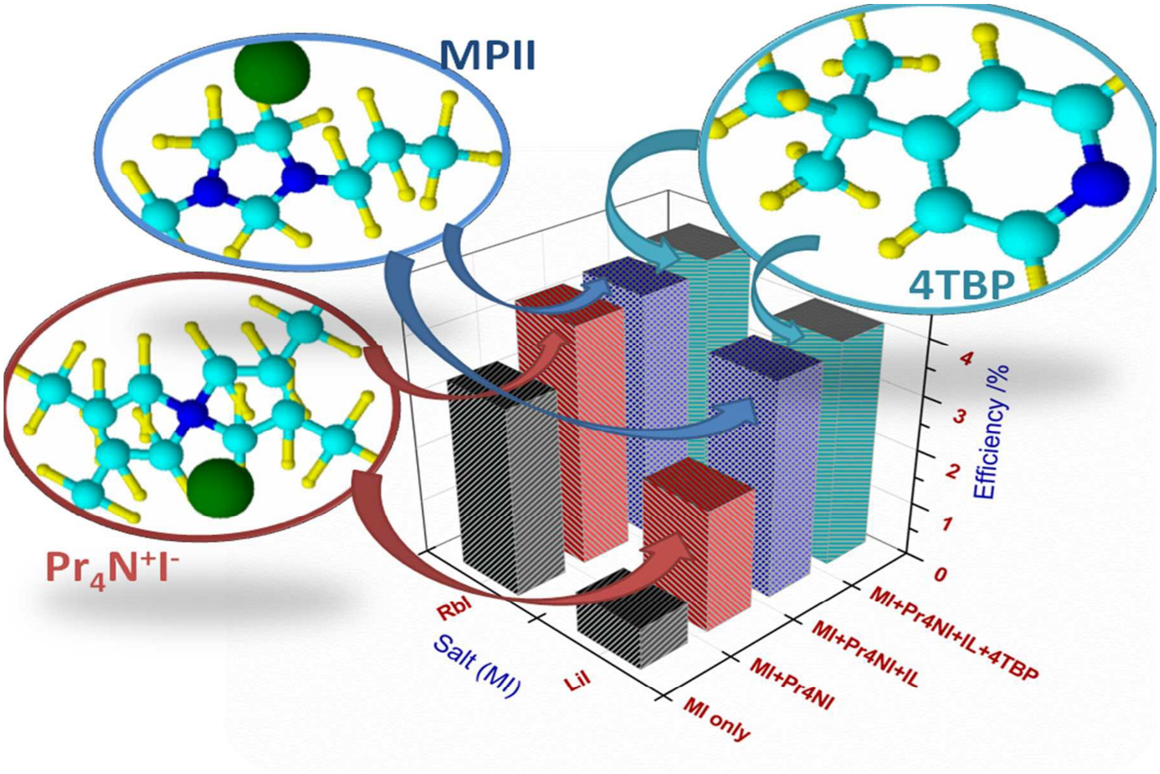

The performance enhancers improved the efficiency in LiI based and RbI based solar cells by 449 and 35.7% respectively.